Modeling the singularity dynamics of a Hele-Shaw flow

J. Elezgaray
Centre de Recherche Paul Pascal, Avenue Schweitzer, 33600 Pessac, France
(Received 17 February 1998)

A simple dynamical model approximating the complex singularity motion of a Hele-Shaw flow is introduced. This model describes accurately secondary tip-splitting instabilities and remains valid for values of the surface tension and time intervals where previous perturbative calculations do not apply.
[S1063-651X(98)06506-4]

PACS number(s): 47.20.−k, 03.40.Gc, 68.10.−m

The time evolution of an air bubble in a Hele-Shaw cell [1] belongs to the wide family of pattern forming systems that can be modeled as Laplacian growth phenomena. Any such system is able to display (in some limit) complex or fractal patterns, the understanding of which remains mostly incomplete. The usual picture is that the asymptotic pattern is reached through a cascade of instabilities (tip splitting or side branching). One expects that simple models for the description of this cascade will shed some light on the underlying dynamical mechanisms generating these complicated patterns. A particularly simple and enlightening example is the branched-growth model introduced in Ref. [2], in the context of diffusion-limited aggregation. The aim of the present work is to introduce a simple dynamical model for the time evolution of the interface of a Hele-Shaw bubble.

We will consider the formulation of the time evolution equations of a Hele-Shaw flow in terms of a conformal mapping $z(\xi,t)$, which maps the interior of the unit circle $|\xi| \leqslant 1$ into the exterior of the bubble, the origin being mapped to infinity. We will also assume the Darcy approximation ($\vec{u} \sim -\vec{\nabla} p$, where $\vec{u}$ is the flow velocity averaged across the cell and p the pressure), the fact that the more viscous fluid is incompressible, while the bubble fluid has zero viscosity and will impose constant flux boundary conditions. The surface tension will be denoted by T. The scaling of all the physical quantities is the same as that of Ref. [7]. Working with a conformal mapping rather than in physical space is particularly convenient in this context, mainly because the Laplace equation $\Delta p = 0$ (implied by the incompressibility) can be easily solved in terms of the Poisson kernel. Historically, this technique was used by Saffman [3] to derive the first family of (finger shaped) exact solutions in the limit of $T=0$. Most of the initial efforts have been devoted to the understanding of the selection of the $\lambda = 1/2$ Saffman-Taylor finger (λ is the ratio of the finger width to the cell width). The solution of this problem [4] has revealed the subtle effect of the surface tension term, which acts as a singular perturbation in the evolution equations.

At any time t for which the interface is regular, the mapping $z(\xi,t)$ is, by construction, analytic in $0<|\xi|\leqslant 1$ but, in general, can develop singularities outside. The motion of the latter is particularly interesting. For instance, when $T=0$ and assuming the singularities to be isolated, it is easy to write their exact evolution equations [5,6]. More generally, it has been shown [7] that, when $T=0$, all the singularities converge towards the unit circle, whereas their singularity exponent α (defined by $\partial_\xi z(\xi,t) \sim A(t)[\xi-\xi_s(t)]^\alpha$) is constant in time. On the contrary, when surface tension is present, Tanveer [7] has shown (assuming $T \ll 1$) that only initial singularities with $\alpha \leqslant -4/3$ preserve this exponent in time. Those (isolated) singularities with $-4/3 < \alpha < -1/2$ are immediately transformed into a ''cluster'' of $-4/3$ branch singularities localized around the initial singularity. Initial zeros of $\partial_\xi z(\xi, t=0)$ also give rise to $-4/3$ singularities (termed ''daughter'' singularities), with the difference that they move with a speed different from that of the original zero, so that their respective trajectories eventually differ. Thus, the existence of initial zeros of $\partial_\xi z(\xi, t=0)$ leads to the strange situation where the $T=0$ and T small solution differ significantly in order $O(1)$ time, even though the $T=0$ solution is regular for any time. This effect has been considered in [8] and [9]. A method to measure the singularity strength has been proposed in [10], where we have directly confirmed the existence of the $-4/3$ singularities.

In this paper a simple dynamical model is presented for the motion of these singularities that works for values of T and time intervals where the perturbative calculations of [7] have been shown to break down. Our initial motivation comes from the consideration of the singularity distributions observed in [10], where we have provided evidence for the existence of ''new'' singularities, that cannot apparently be related to those predicted in the framework of Ref. [7]. Those should be considered as ''second generation'' singularities, in the sense that they appear later than both the initial singularities already present in the initial condition and their possible daughters. In Ref. [10], we also mentioned the existence of $-4/3$ singularities induced by a weak branch cut ($\alpha > 0$) present in $\partial_\xi z(\xi, t=0)$. The model we present here accounts for both of these facts in a simple way and more generally, provides a simple (but approximate) picture of the appearance of secondary instabilities.

We start from the observation that the conformal mapping given by

$$\partial_\xi z(\xi,t) = A(t) \frac{\prod_{i=1}^{N} [\xi - z_i(t)]}{\xi^2 \prod_{i=1}^{N} [\xi - p_i(t)]} \tag{1}$$

is an exact solution of the Hele-Shaw flow equations if $T=0$. Then, $z(\xi,t) = B(t)/\xi + \Sigma_{i=1}^{N} R_i(t) \log(\xi - p_i(t))$. In order to ensure the mapping to be conformal in $0<|\xi|<1$, one

needs to impose $|z_i(t)|>1$, $|p_i(t)|>1$, and $\Sigma_{i=1}^{N} 1/z_i(t) = \Sigma_{i=1}^{N} 1/p_i(t)$. More general forms, allowing, for instance, polynomials of different degrees in the numerator and denominator, can be handled in a similar way. For the sake of simplicity, in this paper we will only consider the particular form (1). The second observation is the fact that, if we identify a fjord (or protrusion) of the interface with an isolated singularity, then the inspection of the time evolution of the shape of a Hele-Shaw bubble shows that an approximation of the type (1) with a *fixed* number of singularities should, *a priori*, be adequate during some interval of time (up to the appearance of additional fjords). Increasing this interval will imply adding more singularities in some rational way that we explain below.

Let us write the evolution equation of the conformal mapping in the form [7]

$$\partial_t \ln z_\xi(\xi,t) = z_\xi^{-1} \partial_\xi (\xi z_\xi I_1(\xi,t)), \tag{2}$$

where

$$I_1(\xi,t) = \frac{1}{2i\pi} \int_{|\xi'|=1} \frac{d\xi'}{\xi'} \frac{(\xi+\xi')}{(\xi'-\xi)} \times \frac{1}{|z_\xi(\xi',t)|^2} \mathrm{Re}[\xi' W_{\xi'}(\xi',t)], \tag{3}$$

and $W(\xi,t)$ is a complex potential such that $\mathrm{Re}[W(\xi,t)]=$ pressure. When $T>0$, the expression (1) is not a solution of Eq. (2), but one can try to find values of the time derivatives $\dot{A}(t)$, $\dot{z}_i(t)$, and $\dot{p}_i(t)$, such that the error estimate

$$E(t) = \frac{1}{2i\pi} \int_{|\xi|=1} |\partial_t \ln z_\xi(\xi,t) - z_\xi^{-1} \partial_\xi (\xi z_\xi I_1(\xi,t))|^2 \frac{d\xi}{\xi} \tag{4}$$

is minimized under the constraint that $\Sigma_{i=1}^{N}[1/z_i(t) - 1/p_i(t)]=0$, for any time t (this approach has been inspired by a similar work [11] for the Burger's equation using the so-called traveling wavelets method). One of the reasons for using the particular form of $z_\xi(\xi,t)$ given in Eq. (1) is the fact that the minimization of $E(t)$ can be done in an analytic way, the details of which will be given elsewhere. One is then led to consider the set of $2N+1$ coupled complex ODE's

$$\mathcal{M}[\dot{A},\dot{z}_1,\ldots,\dot{p}_N]^T = \mathcal{F}, \tag{5}$$

where $\mathcal{M}$ is a square matrix of size $2N+1$, and $\mathcal{F}$ a $(2N+1)$-dimensional vector, both of them being analytic functions of $A(t), z_1(t),\ldots,p_N(t)$. The evolution model we study is the following. First, we choose (arbitrarily) some precision parameter ϵ. For a given initial interface, it is always possible [12] using Padé's method [13] to approximate $z_\xi(\xi,t=0)$ with precision ϵ by an expression of type (1). Let N_0 be the number of couples of singularities (z_i^0, p_i^0) obtained in this way. Their time derivatives are chosen through the minimization of $E(0)$. However, it is likely that $E(0)>\epsilon$, in which case more singularities are needed. One simple method to find them is to perform a Padé analysis of the right-hand side of Eq. (2), evaluated on the unit circle. Notice that the T-independent part of I_1 (such that $\xi W_\xi = -Q/2\pi$, see [7]) has exactly the same singularity structure as z_ξ. As expected, new singularities come into play through the surface tension term of I_1. Let us note by (z_i^T, p_i^T), $i=1,\ldots,N_0'$ the zeros and poles obtained from the Padé analysis of the T-dependent term of the right-hand side of Eq. (2). Then, the initial condition will be written under the form (1), with $N=N_0+2N_0'$, $z_i(0)=z_i^0$, $p_i(0)=p_i^0$, $i=1,\ldots,N_0$, $z_i(0)=z_{i-N_0}^T$, $p_i(0)=z_{i-N_0}^T$, $i=N_0+1,\ldots,N_0+N_0'$, and $z_i(0)=p_{i-N_0-N_0'}^T$, $p_i(0)=p_{i-N_0-N_0'}^T$, $i=N_0+N_0'+1,\ldots,N_0+2N_0'$. This form ensures a correct approximation of both $z_\xi(\xi,t=0)$ and its time derivative.

One of the major weaknesses of the present approach is related to the fact that the minimum of $E(0)$ is not uniquely defined for the above form of the initial condition, but only fixes the values of $\dot{z}_i - \dot{p}_i$, $i=N_0+1,\ldots,N_0+2N_0'$. Thus, an additional condition is needed in order to completely specify the model. Several conditions have been tried, all of them leading to similar conclusions as far as the asymptotic dynamics is concerned. All the examples given below have been done by imposing that, at $t=0$, $\dot{z}_i(t=0)=0$, $i=N_0+1,\ldots,N_0+2N_0'$. Another important point is whether two slightly different interfaces (the exact initial interface and its approximation using Padé approximants) evolve in a similar way. In view of the results of [5], this is probably wrong in general. The examples below show, however, that, for finite intervals of time, their time evolutions are comparable.

Let us first consider an initial interface with exactly two zeros and poles, $z_1(0)=1.4$, $p_1(0)=1.3$, $z_2(0)=1.3\sqrt{-1}$, $p_2(0)$ being determined by $1/p_2(0) = -1/p_1(0) + 1/z_1(0) + 1/z_2(0)$. When $T=0$, $z_2(t)$ reaches the unit circle in finite time ($t\sim 0.6$), and the interface develops a cusp. On the contrary, $z_1(t)$ is screened by $p_1(t)$, and never reaches $|\xi|=1$. The addition of surface tension regularizes the problem as can be seen in Fig. 1(b), where the time evolution for $T=0.01$ and $0\leqslant t\leqslant 28$ is represented. The value of T (which is rather large compared to those considered in Ref. [9]) has been dictated by the wish of studying secondary instabilities in a reliable way [14], as well as exploring parameter regions where the scaling predictions of Ref. [7] do not hold.

The Padé analysis of the T-dependent part of I_1 imposes, at the lowest order, the addition of (respectively) three and four couples of singularities for each of the two initial couples of singularities ($N_0'=7$). Lower values of N_0' yield $E(0)\sim\|\partial_t(\ln z_\xi)\|$. With the addition of these ''new'' singularities, $E(0)\sim 10^{-2}\|\partial_t(\ln z_\xi)\|$. The time evolution (computed with an adaptive time step Runge-Kutta method) of the set of 9 couples of singularities according to the dynamical model Eq. (5) is represented in Fig. 1(a), the corresponding interfaces being represented in Fig. 1(b). The time integration of Eq. (5) stops when the number of points required to evaluate the contour integrals involved in $\mathcal{F}$ exceeds 2^{17}; in this particular case, $t\sim 18$. From Fig. 1(a), it is clear that the singularities tend to organize (asymptotically) into pairs of zeros and poles. Thus, based on the results of Ref. [10], we conclude that the present model approaches a $-4/3$ singularity by a pole ($\alpha=-1$), accompanied by a neighboring zero. Figure 1(b) shows that this approximation is actually quite reasonable [in this picture, the reference (''exact'') solution has been computed using the algorithm of Ref. [15]]. This fact explains, in some sense, the early observations made by Dai *et al.* [16] that the daughter singularities spawned by an

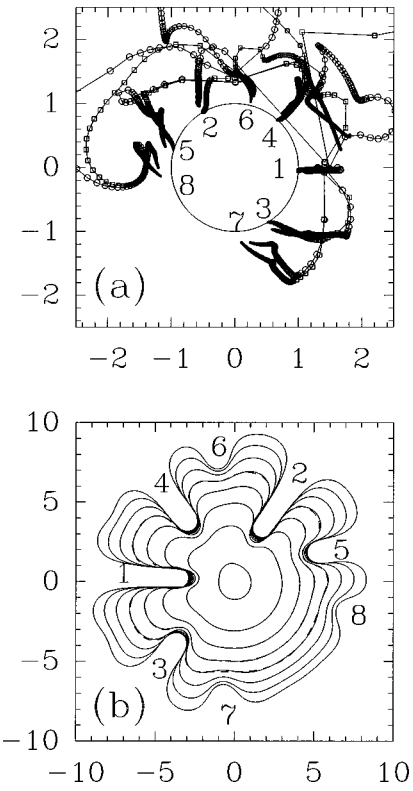

FIG. 1. (a) Time evolution of the nine zero-pole couples approximating the initial condition $\partial_\xi z(\xi,0)=(\xi-1.4)(\xi-1.4\sqrt{-1})/(-\xi-1.3)/[\xi-p_2(0)]/\xi^2$ with surface tension $T=0.01$ [$p_2(0)$ is given in the text]. Zeros (poles) are represented by circle (squares). The symbols belonging to the same trajectory are connected by a continuous line. Their size decreases in time to indicate the direction of the trajectory. (b) Comparison between the reconstructed interfaces (dashed line, $t_{\max}=16$) corresponding to the singularities represented in (a) and the exact interface (continuous line, $t_{\max}=28$), computed with the algorithm of Ref. [15]. The time interval between two consecutive interfaces is $t=4$.

initial zero can be approached (using Domb-Sykes plots, for instance) as polelike singularities. In other words, the shape of a fjord corresponding to a $\alpha=-4/3$ singularity, or that generated by a zero-pole couple, are actually very close. The labeling of the zero-pole couples corresponds to that of Fig. 1(b). The two initial zero-pole couples become the two trajectories marked 1 and 2. Those can be shown to correspond to $-4/3$ singularities using the Fuchs analysis of Ref. [10]. ''New'' trajectories, marked 3, 4, and 5, correspond probably to the daughter singularities of the two initial zeros. The trajectories marked 6, 7, and 8 are typical examples of ''second generation'' fjords. Notice that trajectories 6, 7, and 8 are much further from $|\xi|=1$ than the others (the time evolution of the ''exact'' interface is shown up to $t=24$ in order to stress the fact that trajectories 6 to 8 do eventually correspond to fjords, something not visible at $t=16$).

In Table I, the exact initial distribution of zeroes and poles, and their asymptotic location is given. The asymptotic pairing of zeros and poles does not necessarily correspond to the initial singularity distribution, and may depend on the additional constraint needed to define the minimization of $E(0)$. For instance, z_6 goes to fjord 1, whereas p_6 corresponds, rather unexpectedly, to fjord 3. In contrast to the $T=0$ dynamics, where it can be shown [7] that the radius of any singularity decreases in time, a typical singularity trajectory (when $T>0$) starts with a rather quick increase of the radius (and in some cases of the angular position) followed by a much slower approach of the unit circle. The initial fast motion is critical for the separation of the singularities, and its details depend on N_0'. However, it is remarkable that the asymptotic behavior is mostly independent of N_0'. In other

TABLE I. Initial singularity distribution of Fig. 1(a) (radius and angle refer to the polar coordinates of each singularity), and their asymptotic trajectory [numbered according to Fig. 1(a)]. Notice that the couple (z_9,p_9) is too far from the unit circle to be in correspondence with any fjord.

Singularity	Initial radius	Initial angle (degrees)	Asymptotic trajectory
z_1	1.4	0.0	3
p_1	1.3	0.0	1
z_2	1.4	90.0	8
p_2	1.395876	94.39870	2
z_3	1.331099	89.760048	5
p_3	1.331099	89.760048	5
z_4	1.486233	89.108719	6
p_4	1.486233	89.108719	8
z_5	1.386236	86.821175	4
p_5	1.386236	86.821175	4
z_6	1.300675	0.0862870	1
p_6	1.300675	0.0862870	3
z_7	1.405713	−3.0412028	7
p_7	1.405713	−3.0412028	7
z_8	1.415905	3.34401773	2
p_8	1.415905	3.34401773	6
z_9	1.483946	−0.39628865	9
p_9	1.483946	−0.39628865	9

TABLE II. Initial singularity distribution of Fig. 2(a) (radius and angle refer to the polar coordinates of each singularity), and their asymptotic trajectory [numbered according to Fig. 2(a)].

Singularity	Initial radius	Initial angle (degrees)	Asymptotic trajectory
z_1	1.81	−179.956	1′
p_1	2.20	−179.956	3
z_2	1.805	77.638	2
p_2	7.07	60.3468	2
z_3	1.805	−77.638	2
p_3	7.08351	−60.60	2
z_4	1.03429	−180	1
p_4	1.03429	−180	3′
z_5	1.1369	89.0	3
p_5	1.1369	89.0	1
z_6	1.1371	−88.9	3′
p_6	1.1371	−88.9	1′
z_7	1.2137	60.755	4
p_7	1.2137	60.755	4
z_8	1.21454	−60.745	4′
p_8	1.21454	−60.745	4′

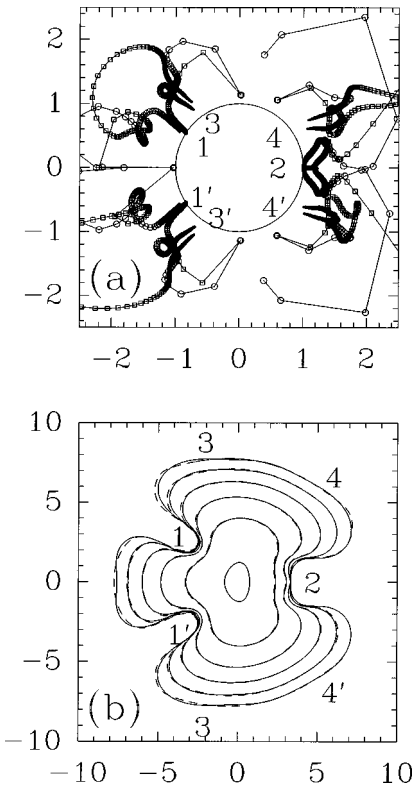

FIG. 2. (a) Time evolution ($t_{\max}=25$) of the eight zero-pole couples approximating the initial condition $\partial_\xi z(\xi,t=0)=(1.2+\xi)^{0.5}+1/\xi^2$, with $T=0.01$. Zeros (poles) are represented by circle (squares). The symbols belonging to the same trajectory are connected by a continuous line. Their size decreases in time to indicate the direction of the trajectory. (b) Comparison between the reconstructed interfaces (dashed line) corresponding to the singularities represented in (a) and the exact interface (continuous line). The time interval between two consecutive interfaces is $t=5$.

words, increasing N_0' preserves the asymptotic behavior of the low generation singularities, and adds higher generations, characterized by the fact that the transient fast motion takes the singularity farther and farther from the unit circle.

In order to study the effect of approximating an initial conformal mapping not of the form (1), let us now consider the time evolution of $\partial_\xi z(\xi,t=0)=(\xi+0.5)^{0.5}+1/\xi^2$. This case has been studied in [10], where we provided evidence for the generation of $\alpha=-4/3$ singularities from the $\alpha=1/2$ initial singularity. Notice that besides the square root singularity, two symmetric zeros exist located at $\xi_0^{\pm}\sim 0.4\pm i1.7$, and that no zeros are present at infinity. The lowest Padé approximant of $\partial_\xi z(\xi,t=0)$ in the form (1) consists of three zero-pole couples, the poles associated to the two zeros $\xi_0^{\pm}$ being located fairly far from $|\xi|=1$ (rigorously, these two poles should be located at infinity). Table II gives the exact initial location of the singularities, as well as their asymptotic location. Applying Tanveer's theory to this new initial condition naturally explains the existence of the two trajectories marked 1 and $1'$ in Fig. 2(a), corresponding to $\alpha=-4/3$ (cf. [10]). Figure 2(b) also shows that the approximation made for the initial interface is quite good, and that it is preserved under the dynamics of the system (5) for a non-negligible interval of time. In fact, the differences observed in Fig. 2(b) between the real interface and that generated by Eq. (5) can be easily fixed by improving the approximation of the curvature-dependent term of I_1.

To summarize, the motion of the complex singularities of a Hele-Shaw flow has been shown to be well approximated, for finite time intervals, by a finite system of coupled ODE's describing the trajectories of pairs of zero poles. This approximation is independent of the value of the surface tension parameter. The clusters of $-4/3$ singularities, predicted in Ref. [7], are approximated by a finite (usually two) number of well defined zero-pole trajectories. Secondary instabilities can be related to the existence of a complex singularity structure induced by the surface tension term around the location of the singularities of $\partial_\xi z(\xi,t=0)$. From this point of view, the tip-splitting phenomenon appears to be a completely deterministic mechanism, resulting from the approach to the unit circle of singularities initially advected far from their original position.

The author acknowledges computer resources from Pôle MNI (U. Bordeaux I), and stimulating discussions with R. Gay, M. Holschneider, A. Arneodo, Y. Couder, and M. Benamar.

[1] D. Bensimon, L. P. Kadanoff, S. Liang, B. I. Shraiman, and C. Tang, Rev. Mod. Phys. **58**, 977 (1986).
[2] T. Halsey, Phys. Rev. Lett. **72**, 1228 (1994).
[3] P. G. Saffman, Q. J. Mech. Appl. Math. **12**, 146 (1959).
[4] R. Combescot, T. Dombre, V. Hakim, Y. Pomeau, and A. Pumir, Phys. Rev. A **37**, 1270 (1987).
[5] S. D. Howison, J. Fluid Mech. **167**, 439 (1986); SIAM (Soc. Ind. Appl. Math.) J. Appl. Math. **460**, 20 (1986).
[6] G. Baker, M. Siegel, and S. Tanveer, J. Comput. Phys. **120**, 348 (1995).
[7] S. Tanveer, Philos. Trans. R. Soc. London, Ser. A **343**, 1 (1993)
[8] M. Siegel and S. Tanveer, Phys. Rev. Lett. **76**, 419 (1996).
[9] M. Siegel, S. Tanveer and W. Dai, J. Fluid Mech. **323**, 201 (1996).
[10] J. Elezgaray, P. Petit and B. Bonnier, Europhys. Lett. **37**, 263 (1997).
[11] C. Basdevant, M. Holschneider and V. Perrier, C. R. Acad. Sci., Ser. I: Math. **310**, 647 (1990).
[12] This is Runge's theorem, see J. B. Conway, *Functions of One Complex Variable* (Springer, New York, 1978), p. 198.
[13] C. Bender and S. Orszag, *Mathematical Methods for Scientists and Engineers* (McGraw-Hill, New York, 1987).
[14] W. Dai and M. J. Shelley, Phys. Fluids A **5**, 2131 (1993).
[15] T. Y. Hou, J. S. Lowengrub, and M. J. Shelley, J. Comput. Phys. **114**, 312 (1994).
[16] W. Dai, L. P. Kadanoff, and S. Zhou, Phys. Rev. A **43**, 6672 (1991).